Sintering of porous hydroxyapatite implant prepared with hybrid fabrication routes

Y.M.Z.Ahmed[1]*, S.M.El-Sheikh[2], Z.I.Zaki[1], E.M.M.Ewais[1]
[1]Ceramic and Refractory Materials Division, (EGYPT)
[2]Nano-structured materials Division, Central Metallurgical Research and Development Institute, CMRDI
P.O. Box: 87 Helwan, 11421, Helwan, (EGYPT)
E-mail: ahmedymz@hotmail.com

ABSTRACT

Porous hydroxyapatite sintered samples possesses suitable chemical, physical and mechanical properties were successfully prepared using combining forming techniques. Starch consolidation (using native potato starch) and pore forming (using hydrogen peroxide) techniques were applied in this concern. The chemical, physical and mechanical properties of the consolidated samples after sintering were studied. The chemical properties of the sintered samples in terms of phase analysis using XRD and FT-IR analysis proves that, while, both potato starch and sintering temperature influence the phase composition of the final sintered samples the hydrogen peroxide addition not show any effect. A hydrogen peroxide amount was found to have a tremendous effect on both physical and mechanical properties of the final sintered samples. The apparent porosity was found to highly increase from ~25% to ~ 70% with increasing the hydrogen peroxide amount from 0 to 5 wt.%, respectively. While, the pore size distribution was found to be highly changed from mono-modal to multi-modal type with increasing peroxide amount from 0 to 5 wt.%, respectively. On the other hand, the compressive strength of the final sintered samples was found to be highly retarded with increasing peroxide amount. For porous samples having higher porosity (with 5 wt.% H_2O_2 addition), beside, it shows a suitable porosity and pore size distribution, it was found to possess a reasonable compressive strength for being applied as implant.
© 2015 Trade Science Inc. - INDIA

INTRODUCTION

About 60 wt.% of bone is made of carbonate substituted apatite $Ca_{10}(PO_4)_6(OH)_{2-2x}(CO3)_x$) therefore it is clear why hydroxyapatite $(Ca)_{10}(PO_4)_6(OH)_2$) and related calcium phosphates have been intensively investigated as the major component of scaffold materials for bone tissue engineering. Calcium phosphates have excellent biocompatibility due to their close chemical and crystal resemblance to bone mineral[1]. Numerous in vivo and in vitro assessments have shown that calcium phosphates, whether bulk,

Full Paper

coating, powder, porous and crystalline or amorphous, always support the attachment, differentiation, and proliferation of osteoblasts and mesenchymal cells, with hydroxyapatites being the most efficient among them[2].

However, despite chemical similarities, mechanical performance of synthetic HA is very poor compared to bone[3]. The formation of tissues with desirable properties relies on scaffold material mechanical properties on both the macroscopic and the microscopic level. Macroscopically, the scaffold must bear loads to provide stability to the tissues as they form while maintaining its original volume. On the other hand, cell growth and differentiation and ultimate tissue formation on the microscopic level are dependent on mechanical input to the cells[4].

Biological studies and clinical practices have established that in addition to the requirements for compositional and the mechanical properties of the material, a 3D interconnected porous structure is necessary to allow cell attachment, proliferation, and differentiation, and to provide pathways for bioûuids. However, it is well known that the mechanical strength of a material generally decreases as its porosity increases. The conûicting interests between biological and mechanical requirements thus pose a challenge in developing porous scaffolds for load-bearing bone tissue engineering[5].

Porous HA exhibits strong bonding to the bone; the pores provide a mechanical interlock leading to a firm fixation of the material. Bone tissue grows well into the pores, thus increasing strength of the HA implant. The ideal bone substitute is a material that will form a secure bond with the tissues by allowing, and even encouraging, new cells to grow and penetrate. One way to achieve this is to use a material that is osteophilic and porous, so that new tissue, and ultimately new bone, can be induced to grow into the pores and help to prevent loosening and movement of the implant[6].

Accordingly, beside the importance of the mechanical properties of the scaffold, most of investigators restricted the application of the calcium phosphate ceramic porous body on the porosity and pore size distribution in the final sintered product. These restrictions have been identified by various investigators depending on the pore size that should be included in the porous body. It is feasible to design the porosity of the materials to be similar to that of trabecular bone, which has a 50–95% of porosity and a network of interconnected pores[7]. In this sense, it is of great interest to obtain pore diameters of a hundred microns[8,9] and a number of designing pore interconnections to verify in the shortest possible time a bioresorption of the scaffold and the subsequent new bone formation. For this purpose, it is necessary to design highly porous scaffolds, which must include the necessary macroporosity to ensure bone oxygenation and angiogenesis[10]. Therefore, designed porous scaffolds should have a network of interconnected pores where more than 60% of pores should have a size ranging from 150 to 400 µm and, at least 20% should be smaller than 20 µm. Pores with sizes of less than 1 µm are appropriate to interact with proteins and are the main responsible for bioactivity. On the other hand, pores with sizes between 1 and 20 µm are important in cellular development, type of cells attracted and orientation and directionality of cellular ingrowth. Moreover, pores of sizes between 100 and 1000 µm play an important role in cellular and bone ingrowth, being necessary for blood ûow distribution and having a predominant function in the mechanical strength of the substrate. Finally, the presence of pores of sizes greater than 1000 µm will have an important role in the implant functionality and in its shape and esthetics.

Consequently, porosity of three-dimensional scaffolds is a very important matter due to its great influence on the implant final behavior. Accordingly, a number of bioceramics fabrication techniques have been proposed. There are replica technique, e.g. replamineform and PU impregnation[11,12], sacrificial template technique, e.g. dual-phase mixing and camphene-based freeze casting[13,14] and direct foaming technique, e.g. foaming method, starch consolidation and gelcasting[15,16,17]. However, almost previous studies were based on using a single technique. A few works focused on porous fabrication using a combination of these techniques. Padilla et al[18]. studied on porous HA using a combination of PU impregnation (replica) and gelcasting (direct foam-

ing) techniques; and Batulli et al[19]. studied on po-rous zirconia using polyethylene sphere as a sacrificial template and gelcasting techniques. In spite of these, it seems no study on the fabrication of porous HA using combination of starch consolidation technique with pore forming technique have been performed. Herein trials have been made in combining both of these techniques for fabricating a 3D hydroxyapatite sintered body achieving the full requirements of implant applications from its chemical, physical and mechanical point of views. This includes the phase composition, the pore size distribution as well as the compressive strength of the final sintered body. In this concern, hydrogen peroxide, have been added in different weight percentage (based on the total solid content) on slurry prepared from HA powder with 10% potato starch.

EXPERIMENTAL PROCEDURES

Materials

The hydroxyapatite powder used in this investigation was delivered by Riedel-de Haen Co., Seelze, Germany. The bulk characteristics, which are taken from the manufacturer, indicated that the powder only contains minor amounts of compounds other than calcium and phosphates. A stock of the powder was calcined at 1100 °C.

The dispersant applied in this investigation was Acumer 9400 supplied by The Dow Chemical Company, Midland, Michigan, USA. It is a water soluble sodium salt polymer used to disperse and stabilize high-solid mineral slurries. It is an anionic dispersant of sodium polyacrylate polymer (SPA) with the solid content of 41–43 wt.% and molecular weight of 3000–4000 g/mol. The amount of SPA was fixed during the preparing of various HA suspensions (with and without corn starch) at 0.36 wt.% based on the total weight of hydroxyapatite. The temperature of heat treatment (1100 °C) and amount of dispersing agent (0.36 wt.%) were found to be optimal for

preparing well dispersed HA suspensions according to the separate study currently submitted for publication elsewhere.

The commercial potato starch used in this work was supplied by El-Gomhoria Company, Egypt. This starch had no physical or chemical modifications. It was selected primarily due to its low price and easy reproducibility.

The physical properties of both hydroxyapatite powders (as-received and heat treated) and corn starch in terms of density and surface area are shown in TABLE 2.

Processing

Suspensions from both hydroxyapatite powders heat treated at 1100 °C were prepared by adding the predetermined amount of powder gradually to a predetermined amount of bi-distilled water under continuous stirring. The amount of Acumar required to stabilize the HA particles (0.36 wt.% based on the total weight of hydroxyapatite) was dissolved in bi-distilled water and then added to the suspensions. The pH of all suspensions was adjusted at 11. The solid loading of all suspensions was adjusted at 59 vol.%. Afterwards, the suspensions were mixed in a planetary mill for 24 h using zirconia balls to avoid the agglomeration[20] and to allow the deflocculant to adsorb onto the particle surfaces. The volume of suspension was kept as the twice of the total volume of the balls to avoid grinding of powder during mixing[21]. The HA suspensions (of 59 vol.%) were then transferred into a new pots and 10vol.% of potato starch was added and mixed under vigorous contentious mechanical stirring for 3 h to ensure the homogenization of the suspensions. The total solid loading (HA and potato starch) of all suspensions was kept constant at 59 vol.%. Regarding that the potato starch powder has lower density than hydroxyapatite powder (TABLE 1). The adjustment of the solid loading was achieved via the addition of predetermined amounts of distilled water during the addition of potato starch to the HA suspension. After 3 h

TABLE 1 : Properties of as received hydroxyapatite powder, calcined HA powder and potato starch

	As received powder	Powder calcined at 1100ºC	Potato starch
Density, g/cm^3	3.156	3.156	1.45
Surface area, m^2/g	73.867	1.895	0.666

Full Paper

of vigorous mechanical stirring for homogenization and conditioning the suspensions, various amount of hydrogen peroxide ranged from 0.2 to 5 wt.% (based on the total solid weight) was then added to the prepared slurry with mild stirring for 10 min. The slurry is then ready for casting. After casting the suspensions into non-porous moulds (Teflon), they were heated in a dryer at 80 °C for 24 h. The drying process was carried out in an ordinary dryer oven Carbolite Fan Convection Oven (Hope Valley, UK) with a heating rate of 5 °C/min. According to the fact that the potato starch gelatinization started at 50-56 °C and ended at 68 °C[22,23]. Also, at 60ºC the decomposition of H_2O_2 produced the foam of the paste[24]. The drying temperature of all samples was fixed at 80 °C throughout the investigation.

The produced green samples were then subjected firstly to binder removal prior to sintering step. The removal of starch was performed in a muffle furnace (Nabertherm, Germany) at a controlled heating rate to prevent blistering, cracking, or delamination that would be caused by (i) a mismatch of thermal expansion between the HA and organic phase or (ii) the expansion of exhaust gases. Then the sintering of the green samples was performed in the same furnace. Sintering in the conventional programmable furnace is the most practical and simple procedure. The main problem associated with this method is the generation of thermal and residual stress fields due to low heat conductivity and high shrinkage of the HA. It may lead, in particular, to the formation of micro- and macrocracks in the specimen. To avoid this problem, the temperature ramp (depending on the sample size) usually should not exceed 5æ%C/min. The green samples were sintered at 1350ºC for 2 hrs, while, the furnace reaches these sintering temperatures with a heating rate of 5ºC/min.

Characterizations

X-ray diffraction (XRD, Bruker axs D8, Karlsruhe, Germany) with Cu-K$_\alpha$ ($\lambda = 1.5406$ Å) radiation and secondary monochromator in the 2θ range from 20 to 100° was used to identify the formed phases and determine the crystallite size of the produced powder. The functional group analysis was performed by Fourier transform infrared spectros-

copy (FT-IR). The measurements were carried out in the transmission mode in the mid-infrared range (400–4000 cm^{-1}) at the resolution of 4 cm^{-1}. The studies were performed using the instrument JASCO 3600, Tokyo, Japan. For FT-IR measurements, KBr pellets containing the exact weighted amount of the examined substance were prepared. Morphology of sintered samples was examined using scanning electron microscope (JEOL-JSM-5410 Tokyo, Japan) equipped with EDX unit (England, Oxford, ANCK).

The apparent porosity for sinter samples were determined by Archimedes immersion techniques, whereas, the linear change of sintered samples was determined by common means[25]. The measurement was performed on a five sintered specimens. The pore size distribution was determined by Hg-intrusion porosimeter (Poresizer 9320, Micrometrics, USA).

Since, bioceramics are very brittle, it is very difficult to make the desired shape needed for mechanical characterization by different machining method. Therefore, conventional methods of mechanical characterization such as biaxial, tensile, and impact testing are not applicable to porous bioceramics. Instead, the compression test has been widely applied for characterization of porous scaffolds. For this purpose, samples consisting of cylindrical bars (12 mm in diameter and 12 mm in length) were selected and the compressive tests were performed at a crosshead speed of 0.5 mm/min using a universal testing machine. The compressive strength was evaluated from the maximum point of the stress/strain graph, which occurs when the first crack appeared in the samples. The average of three samples was taken as the measure of the compressive strength of the sample.

RESULTS AND DISCUSSION

XRD and FT-IR analysis

The phase composition of the sintered samples produced from consolidated HA slurry with and without peroxide addition was investigated via XRD and FT-IR analysis. The analysis was performed in order to evaluate the effect of sintering procedure as well as the peroxide amount on the type of phase
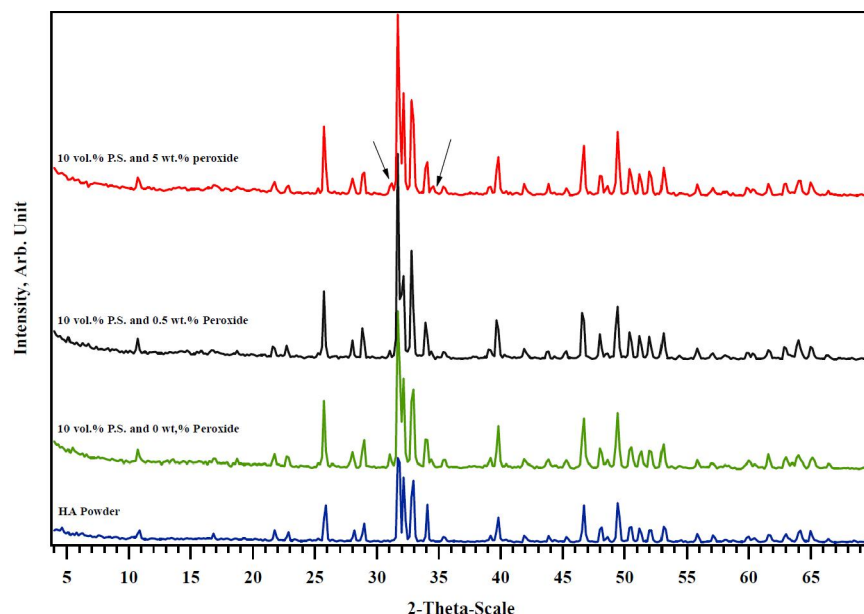
Figure 1 : XRD patterns for HA powder and samples containing 10 vol.% potato starch with and without peroxide addition

formed after sintering.

Figure 1 shows the X-ray diffraction patterns for porous hydroxyapatite samples produced from the sintering of a consolidated slurry contained 10 vol.% potato starch with and without different amount of hydrogen peroxide. After sintering, specimens had been crushed and the powders were examined by X-ray diffraction method. For comparison the XRD pattern of the starting powder was inserted in all graphs. It is clear that, the starting HA powder (which is already calcined at 1100ºC) shows a diffraction pattern in which all peaks is corresponded solely to hydroxyapatite phase (JCPDS 9-432). In contrary, the patterns of samples produced with 10 vol.% potato starch with and without peroxide addition show an additional peaks (assigned by the black arrow in the figure) beside the main phase of hydroxyapatite. These additional peaks were identified as corresponding to β-TCP phase (JCPDS 9-169).

However, the appearance of the additional peaks corresponding to β-TCP is believed to be according to the dissociation of hydroxyapatite during sintering. This dissociation may result from two main reasons. Firstly, it may be related to the applied sintering temperature. Several authors[26,27] have reported on the temperature dependency of HA stability; which could lead to the dissociation of the HA according to the dehydroxylation behavior of HA forming a

nonstoichiometric phase based on the following reaction:

$$Ca_{10}(PO_4)_6(OH)_2 \rightarrow$$
$$Ca_{10}(PO_4)_6O_x(OH)_{2(1-x)} + xH_2O$$
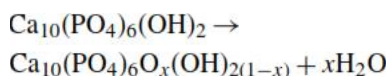
In this reaction, the water is liberated from hydroxyapatite gradually and hydroxyoxyapatite $Ca_{10}(PO_4)_6O_x(OH)_{2(1-x)}$ (HOA) with a gradually decreasing content of OH groups is formed before oxyaptite. This dehydroxylation process is reversible, has no significant effect on the crystal structure of HA and upon attainment of the critical temperature, 75–80% of the bonded water remained[28]. If the critical point is exceeded, complete and irreversible dehydroxylation occurs, resulting in the decomposition of the HA to anhydrous TCP[29]. However, there are disagreements about this critical temperature of HA decomposition, the reasons mainly involving different powder characteristics and firing conditions[26]. Generally, the sintering of HA is highly complicated, while some authors revealed that HA will decompose to anhydrous calcium phosphates such as tricalcium phosphate (TCP) in the range of 1200–1450æ%C[29,30]. This explains the appearance of the β-TCP in all sintered specimens. Secondly, the presence of carbonate ions in the reaction media may be another reason for HA decomposition. The presence of carbonate ions in the apatite structure weakens the bonds, increases the dissolution rate

Full Paper

and the solubility[31]. So the higher amount of carbonate content seems to destabilize the apatite structure leading to the formation β-TCP phase with the presence of HA phase[32]. During sintering of consolidated specimens, a considerable amount of carbonate ions is released as a result of starch evaporation, enhancing HA decomposition. One or even both of the above mentioned reasons could responsible for the partial dissociation of the main HA phase into β-TCP phase in the final sintered samples. It is worth mentioning that, patterns of sample sintered from consolidated slurries with and without peroxide addition is approximately typical. This reveals that addition of peroxide during green samples formation have no effect on the phase composition of the final sintered samples.

The FT-IR analysis for all samples produced from sintering of consolidated HA slurries with and without peroxide addition was carried out and the produced spectra were carefully analyzed. Figure 2 shows the FT-IR spectra of these samples as well as that corresponding to the starting HA powder which inserted as a matter of comparison. Although there are some common features of the spectra produced from various samples some differences between these spectra are clearly noticeable.

The common features are

1. Appearance of absorption bands in the range of ~964, 1045, and 570 cm^{-1}, which are characteristic bands of crystallized apatite phase[33].
2. All vibration modes of PO_4^{3-} (v_1, v_2, v_3, and v_4) are clearly identified in all spectra. Bands appeared at ~964, 470, 1045-1095, and 570-605 cm^{-1} are characteristic bands for v_1, v_2, v_3, and v_4 starching modes of PO_4^{3-} ions, respectively.
3. Bands at 3444 and 1635 cm^{-1} are relevant to the bending modes of hydroxyl group in the absorbed water. While, bands at 3571 cm^{-1} as well as 633 cm^{-1} are assigned to the stretching vibration of hydroxyl group in the crystal structure of hydroxyapatite[34-36].

On the other hand, the most important differences between the observed spectra is that the peak area of the band ~3571 cm^{-1} (assigned for stretching mode of hydroxyl group). This peak was found to be highly decreased from the spectra related to the starting powder to that related to sample produced with 10 vol.% potato starch without peroxide addition. Moreover, the other stretching hydroxyl band which appears at 630 cm^{-1} (in the starting powder spectra) was found to be completely disappeared with sample produced with 10 vol.% potato starch without peroxide addition. These two observations confirm the formation of tri-calcium phosphate, the dehydrated
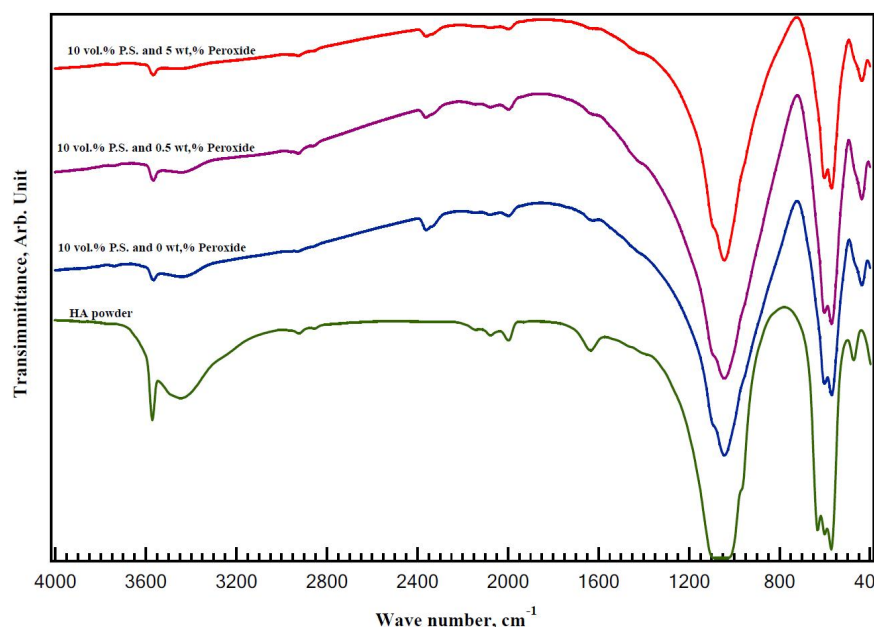
Figure 2 : FT-IR spectra for HA powder and samples containing 10 vol.% potato starch with and without peroxide addition

version of hydroxyapatite, leading to the formation of bi-phasic calcium phosphate[32]. While, no recognized difference is noticed between the spectra of samples sintered from consolidated slurries containing 10 vol.% potato starch with and without peroxide addition. The FT-IR spectra analysis results are in a good agreement with the finding in phase composition change from XRD analysis.

Since calcium phosphate is a biodegradable and bioactive phase. The presence of other calcium phosphate phases together with HA can change biological properties (cellular response and solubility in human blood); for an example, the solubility of calcium phosphate materials increases in the order of HA < β-TCP <α-TCP[37]. HA is stable in a body fluid, whereas TCP is rather soluble in the fluid[38]. Many studies have indicated that the dissolution of well-crystallized HA in the human body after implantation is too low to achieve optimum results. On the other hand, the dissolution rate of β-TCP ceramics is too fast for bone bonding[11]. According to Ducheyne and Qiu[39] how stated that the more soluble the material, the higher the tendency to induce precipitation of bone-like apatite, which effectively contributes to bone formation. This is a consequence of the body fluid enrichment on calcium and phosphorus due to the calcium phosphate dissolution[39]. In accordance, the presence of TCP in the sintered sample it is not undesirable, but in bone tissue engineering and even in drug delivery application is regarded as a benefit phase[40].

Green and sintered samples morphologies

Figure 3 shows the feature of the green samples prepared with different amount of hydrogen peroxide addition. It easily notices that the porosity of the green sample is highly increased with increasing the amount of hydrogen peroxide added. Also the pore diameter is sharp increased with increasing hydrogen peroxide. In addition, it is worthy mentioned that, even with highly porous sample (5 wt.% H_2O_2) the sample is easily handled without any degradation. The high porosity in the produced dried samples with the addition of H_2O_2 solution is a result of the gas voids introduced in the green sample when it was stored at 80°C. It was earlier stated that even
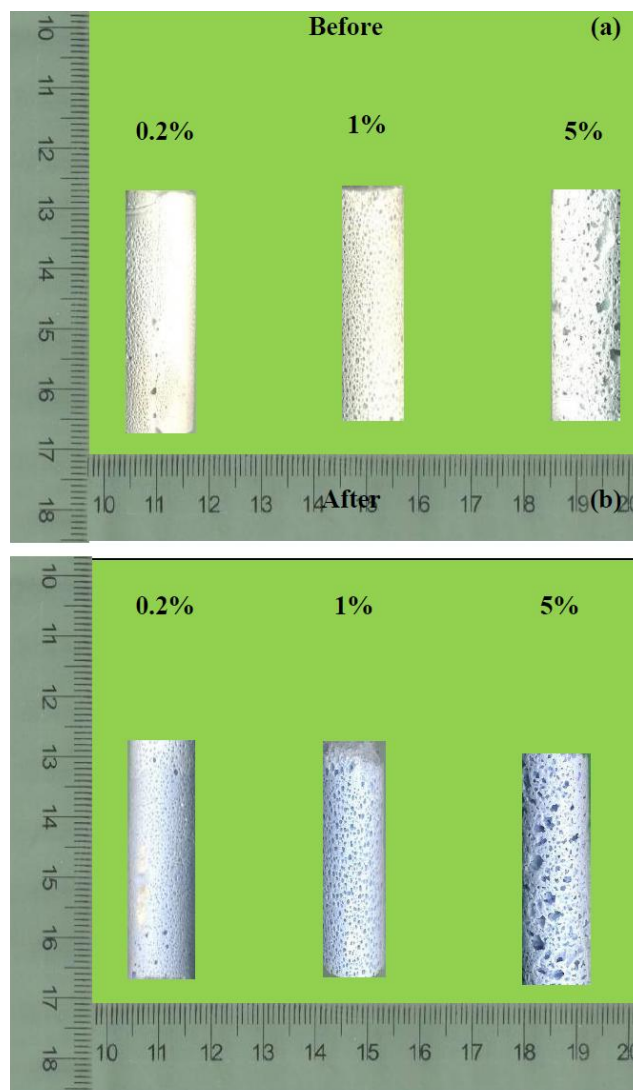

Figure 3 : Photographs of consolidated samples prepared with the addition of different peroxide amount before (a) and after (b) sintering

with the addition of a small amount of hydrogen peroxide solution, considerable voids is introduced in the final dried sample[15]. At elevated temperature (80°C) H_2O_2 could produce H_2 and O_2 gases, leading to the voids in the ceramic body. The gas voids were driven out by heating during the liquid phase. After drying process, the gas voids remaining in the paste became the pores in porous dry bodies[24]. Almirall et al[15]. have been stated that, the H_2O_2 solution resulted to be an effective foaming agent for the calcium phosphate ceramic (CPC). It allowed for the introduction of a high percentage of macroporosity in the material without the addition of second phases or additives which could hinder

Full Paper

the setting reaction of even compromise the excellent biocompatibility and bioactivity of the CPC.

On the other hand, the feature of the samples after sintering is shown in Figure 3b. It is important to notice that the sintering was occurring in all samples without any deformation, which is an indication for the good homogeneity of the green samples[41]. Compare Figures 3a with 3b indicating that the sintering process has largely influenced the sample porosity as well as the pore diameter of the sintered samples. This was expected as a result of evaporating the volatile materials from the sample interior with heat treatment. In addition, all sintered samples were found to have a highly rough surface, which is an advantage for the produced samples. When macroporous ceramics are used as implant, several investigators have confirmed that osteoblast prefer a rough surface[42]. When used as bone tissue engineering scaffold, the surface micropattern plays an important role in regulating the cell/material interaction after seeding[18]. However, the produced porous sintered samples are subjected for various characterizations from physical and mechanical points of views.

Porosity, pore size distribution and SEM analysis

The effect of different hydrogen peroxide amount addition during green sample formation on the apparent porosity as well as the linear change of the final sintered samples was shown in Figure 4.

A sharp increase in the sample porosity is clearly noticeable when the amount of peroxide added increased. Even with a very small addition of peroxide (0.2 wt%) the produced porosity is approximately two fold of a sample without peroxide addition. The maximum apparent porosity of about 70% was obtained with the addition of 5 wt% H_2O_2. On the other hand, no significant change in the linear change of all samples with and without peroxide addition was noticeable. This indicates that, large pores diameter which does not contract during sintering (according to the sintering theory) were formed with the peroxide addition.

The pore size distribution curves of sintered samples produced without and with various amounts of hydrogen peroxide addition during green sample formation were given in Figure 5a-d. It revealed that, hydrogen peroxide addition affected to a large extent the pore diameter created in the final sintered samples. With 0.2 wt.% H_2O_2 addition, approximately bimodal pore size distribution was found (Figure 5b). The pore diameter is ranged from about 10 μm and higher. This feature is completely different if this sample compared with the sample having 10 vol.% potato starch without H_2O_2 addition (Figure 5a). The comparison revealed that addition of peroxide not only increases the diameter of pores in sintered sample but also is responsible for the creation of different pore diameters. However, with increasing peroxide addition (at 1 wt.%) a multimodal pore size distribution were produced, where the pore diameter is shifted to a larger pore size (Figure 5c).
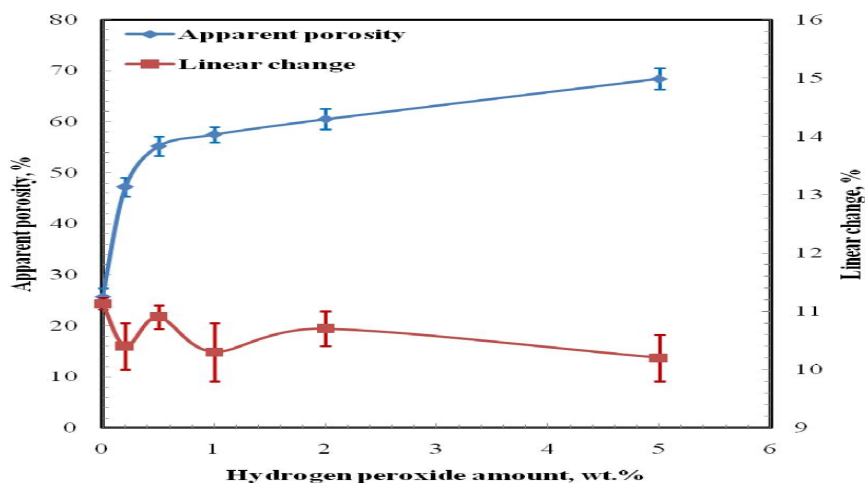

Figure 4 : Effect of addition different amounts of hydrogen peroxide on the apparent porosity and linear change of sintered hydroxyapatite samples
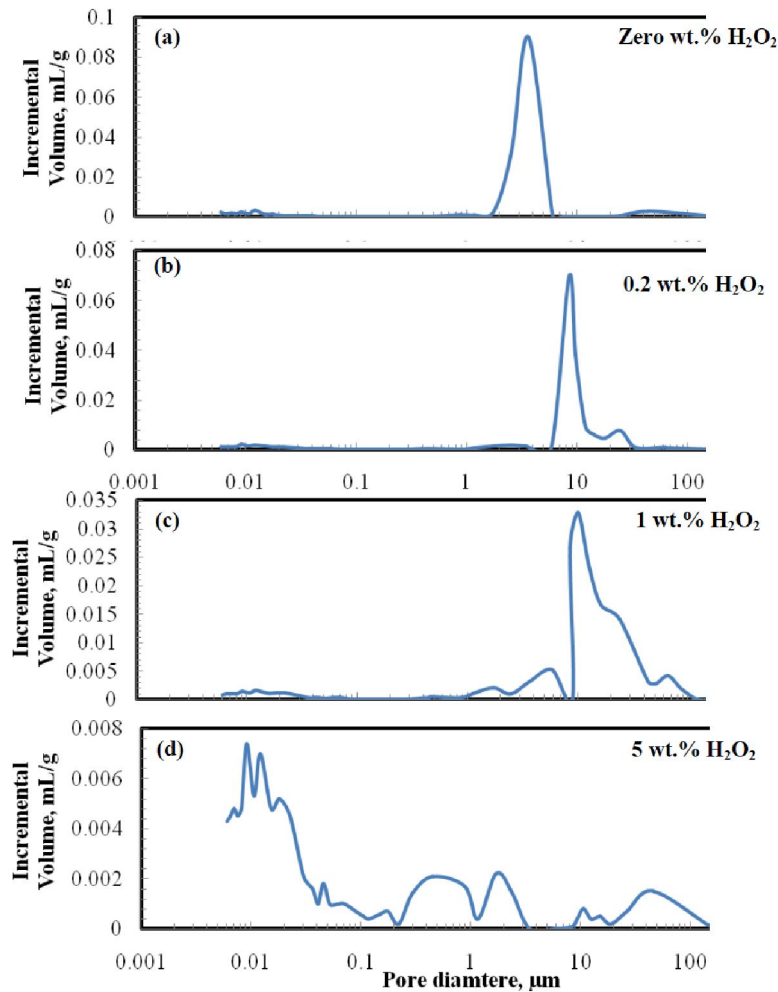
Figure 5 : Pore size distribution of porous samples containing different hydrogen peroxide amounts

This observation is repeated with increasing the peroxide to 5 wt.% (Figure 5d). At 5 wt.% addition a multimodal pore size distribution was also obtained with a homogeneous pore distribution. However, the reason of creation multimodal pore size distribution with the addition of hydrogen peroxide is related to the fact that with H_2O_2 addition, there are various mechanisms responsible for the creation of pores inside the sintered samples. The evolution of the rest of hydrogen peroxide from the sample interior during sintering, the contraction of the small pores created as a result of some water evaporation from the sample interior, the evaporation of the starch granules, and setting of the HA granules during sintering which is also creating some intrinsic porosity in the range of micropores. On the other hand, the presence of a considerable amount of micropores (pores with size lower than 1 μm) is an advantage in the produced sintered samples. Many investigators have revealed that the presence of the interconnected micropores is important to allow the flow of body fluid between the macropores, e.g. the supply of nutrition, and subsequently promote the growth of hard tissue into the macropores[43-45]. Additionally, microporosity further increases the surface area, leading to greater protein adsorption, and thus potentially increased bone ingrowth throughout the specimen, as well as to ion exchange and bone-like apatite formation by dissolution and reprecipitation, as occurs on placing a bioactive material in either a simulated body fluid[46] or the human body[47,48]. On the other hand it was reported that porous ceramic with bimodal pore size distribution[49,50] or even a porosity gradient is simulating the structure of natural bone (cortical and cancellous)[51]. Herein the hydrogen peroxide addition leads to fabricate a sintered HA body having different pore sizes ranged from micro to macrometer pore diameters which is

Full Paper

simulating the natural bone structure. On the other hand, the pore size distribution curves indicated that the incremental volume percentage (which gives indication of the porosity degree) is continuously decreased with increasing the peroxide addition from 0 wt% (Figure 5a) to 5 wt% (Figure 5d). In contrary, the apparent porosity was found to be sharply increased with increasing the amount of peroxide addition. This is good indication that the increasing peroxide addition leads to a creation of pores having a diameter larger than 200 μm which could not be detected with porosimeter instruments[52]. Accordingly, this interpretation could be improved via investigated the samples with a scanning electron microscope.

The scanning electron micrographs of sintered samples produced from consolidated slurries containing 10 vol.% potato starch without and with dif-

ferent hydrogen peroxide addition were shown in Figure 6. It is clearly noticed that increasing the amount of peroxide added leads to a high increase in both porosity and pore size diameter of the final sintered samples. Almost spherical pores were observed with sample produced with 0.2 and 1wt.% peroxide addition (Figure 6c-d, Figure 6e-f) which is completely changed to be irregular in shape with 5 wt.% addition (Figure 6g-h). Most of the produced pores (whatever the peroxide amount) were found to be large and interconnected. Also the large pore produced is contained a huge number of small pore as indicated from the high magnifications photo for all samples (Figure 6d, 6f, 6h). In addition, a large difference was clearly noticeable if the samples with peroxide addition are compared with that produced without peroxide addition (Figure 6a-b). The addition of peroxide enhances to a large extent the cre-
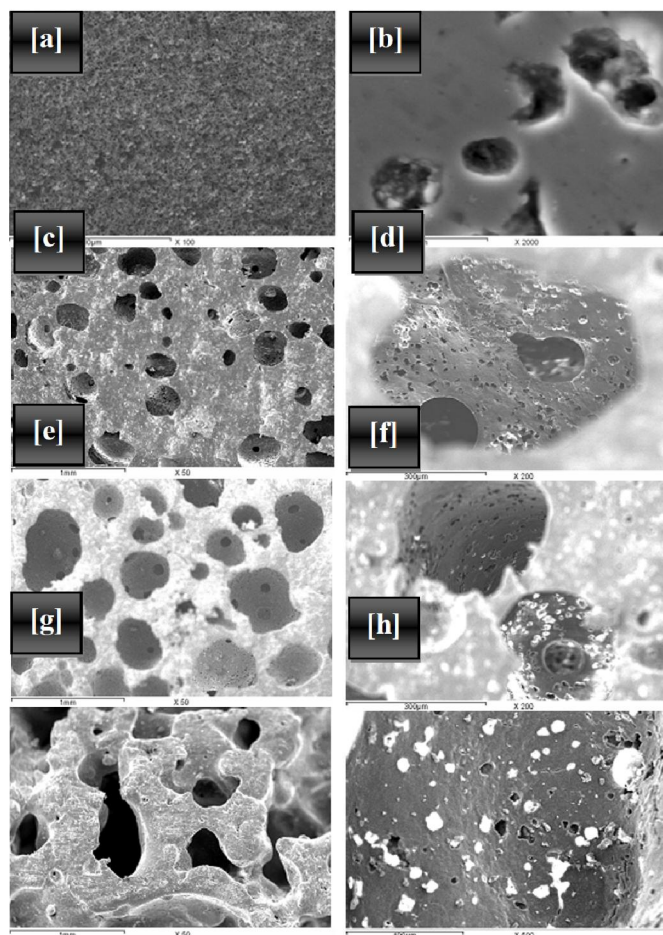

Figure 6 : Scanning electron microscope for sintered samples produced with various hydrogen peroxide additions. [a] & [b] low and high magnifications of sample with 0.2 wt% H_2O_2, [c] & [d] low and high magnification of sample with 1 wt% H_2O_2, [e] & [f] low and high magnification of sample with 5 wt% H_2O_2

ation of large pore with huge amounts. Also from these figures, it could be easily noticed that for samples produced with various peroxide addition, most of the pores diameter were exceeding the 200 mm which is the limit of porosimeter apparatus to be detected. This confirms the conclusion deduced from pore size distribution (Figure 5) that the amount of incremental volume decreased with increasing the peroxide addition as a result of creation pore diameter larger than that could be detected with porosimeter apparatus.

Compressive strength

The compressive strength of the sample produced from sintering of consolidated HA slurries containing 10 vol.% potato starch without and with various amounts of hydrogen peroxide addition was shown in Figure 7. A dramatic decrease in the compressive strength of the sintered samples is clearly noticeable with the addition of peroxide during green sample formation. The retardation of the compressive strength is due to the large increase in both the sample porosity and the diameter of created pores with increasing the amount of peroxide added during green sample formation.

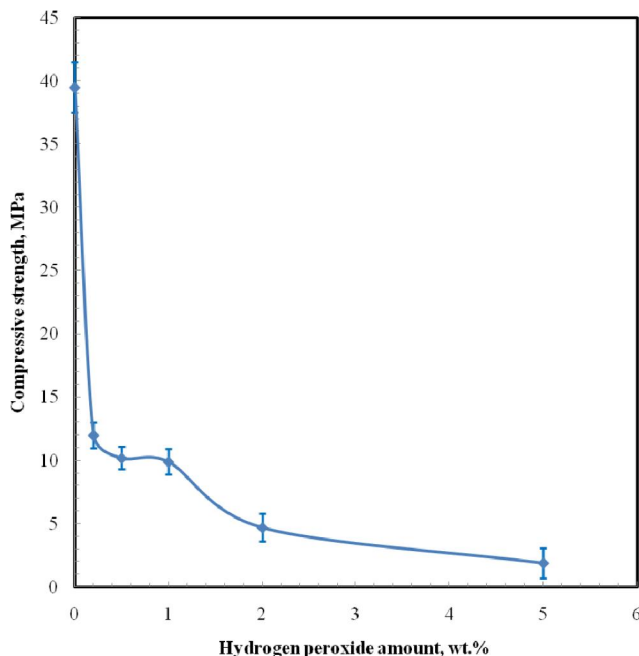It is well known that the pore architecture of the

implant directly affects its mechanical strength[17]. Since, a higher density usually leads to higher mechanical strength, high porosity provides a favorable biological environment. Therefore, a balance between the porosity and density for the implant must be established for the specific application[53]. The minimum compressive strength for the prepared implant was determined as 1.9 MPa (for sample with 5 wt.% peroxide addition), which is somewhat close to the strength of natural bone[54]. The compressive strength of porous human bone ranges between 2-12 MPa for cancellous bone and 100–230 MPa for cortical bone[38]. This means that the as-prepared artiûcial porous HA with highest apparent porosity and excellent pore size and pore size distribution (with the addition of 5% H_2O_2) possesses the minimum compressive strength required for implant application. It is worthy to mention that after implantation bone ingrowth lead to the enhanced compressive strength of porous implants. Even for low density implants this observation is more obvious due to faster bone growth[55]. The compressive strength of porous HA, for example, was reported to increase from 2 to 20 MPa after 3 months implantation[56].

CONCLUSIONS

Starch consolidation combined with pore forming techniques was found to be a beneficial way for fabricating sintered porous HA samples having the requirements for implant application. The addition of potato starch influenced the chemical composition of the starting HA powder after sintering while; H_2O_2 addition during green sample formation has no effect in this concern. Partial dissociation of the parent HA phase into β-TCP one is recorded for all sintered samples produced from consolidated HA slurries containing 10 vol.% potato starch without and with various amounts of H_2O_2 addition. The addition of peroxide was found to not only responsible for increasing the apparent porosity of the sintered samples from about 25 to 70%. But also is responsible for changing the pore morphology from spherical to irregular as well as the pore size distribution from mono modal to multimodal type with increasing peroxide addition from 0 to 5 wt.%, re-

Figure 7 : Effect of addition different amounts of hydrogen peroxide on the compressive strength of sintered hydroxyapatite samples

Full Paper

spectively. A large reduction in compressive strength from about 39 to 2 MPa with increasing peroxide addition from 0 to 5 wt.%, respectively is a reflection for increasing both apparent porosity and pore diameter of the final sintered samples. Obviously, the produced sintered sample with the addition of different percentage of hydrogen peroxide, especially the one produced at highest peroxide addition fulfills all requirements for the applications of this sample as implant.

ACKNOWLEDGEMENTS

REFERENCES

[1] E.Sahin; "Synthesis and characterization of calcium phosphate cement based macroporous scaffolds," Ph.D. Thesis, Graduate School of Engineering and Sciences of Izmir Institute of Technology, Izmir, Turkey, **(2012)**.

[2] K.Rezwan, Q.Z.Chen, J.J.Blaker, A.R.Boccaccini; "Biodegradable and bioactive porous polymer/inorganic composite scaffolds for bone tissue engineering," Biomaterialsm, **27**, 3413-3431 **(2006)**.

[3] A.I.Itala, H.O.Ylanen, C.Ekholm, K.H.Karlsson, H.T.Aro; "Pore diameter of more than 100 micron is not requisite for bone ingrowth in rabbits," J Biomed.Mater.Res., **58**, 679–83 **(2001)**.

[4] J.L.Drury, D.J.Mooney; "Hydrogels for tissue engineering: scaffold design variables and applications," Biomaterials, **24** 4337-4351 **(2003)**.

[5] H.R.Ramay, M.Zhang; "Preparation of porous hydroxyapatite scaffolds by combination of the gelcasting and polymer sponge methods," Biomaterials, **24**, 3293–3302 **(2003)**.

[6] S.K.Swain; "Processing of porous hydroxyapatite scaffold," Master of Technology Thesis, Department of Ceramic Engineering, National Institute of Technology, Rourkela, India, **(2009)**.

[7] M.Doblar, J.M.Garcia, M.J.Gomez; "Modelling bone tissue fracture and healing: a review," Eng.Fract.Mech., **71**, 1809–40 **(2004)**.

[8] J.J.Klawitter, S.F.Hulbert; "Application of porous ceramics for the attachment of load bearing orthopaedic applications," J.Biomed.Mater.Res.Symp., **2**, 161–229 **(1971)**.

[9] O.Gauthier, J.M.Bouler, E.Aguado, P.Pilet, G.Daculsi; "Macroporous biphasic calcium phosphate ceramics: influence of macropore diameter and macroporosity percentage on bone ingrowth," Biomaterials, **19**, 133–39 **(1998)**.

[10] M.Vallet-Regi; "Revisiting ceramics for medical applications," Dalton Trans., 5211–5220 **(2006)**.

[11] S.H.Kwon, Y. K. Jun, S. H.Hong, I.S.Lee, H.E.Kim; "Calcium phosphate bioceramics with various porosities and dissolution rates," J.Am.Ceram.Soc., **85(12)**, 3129–31 **(2002)**.

[12] D.C.Tancred, B.A.O.McCormack, A.J.Carr; "A synthetic bone implant macroscopically identical to cancellous bone," Biomaterials, **19**, 2303-11 **(1998)**.

[13] E.J.Lee, Y.H.Koh, B.H.Yoon, H.E.Kim, H.W.Kim; "Highly porous hydroxyapatite bioceramics with interconnected pore channels using camphene-based freeze casting," Materials Letters, **61**, 2270–3 **(2007)**.

[14] S.H.Li, J.R.de Wijn, P.Layrolle; "Novel method to manufacture porous hydroxyapatite by dual-phase mixing," Journal of the American Ceramic Society, **86**, 65-72 **(2003)**.

[15] A.Almirall, G.Larrecq, J.A.Delgado, S.Martínez, J.A.Planell, M.P.Ginebra; "Fabrication of low temperature macroporous hydroxyapatite scaffolds by foaming and hydrolysis of an α-TCP paste," Biomaterials, **25**, 3671-80 **(2004)**.

[16] Y.M.Z.Ahmed, E.M.M.Ewais, S.M.El-Sheikh; "Eûect of dispersion parameters on the consolidation of starch-loaded hydroxyapatite slurry," Processing and Application of Ceramics, **8**, 127–135 **(2014)**.

[17] P.Sepulveda, F.S.Ortega, M.D.M.Innocentini, V.C.Pandolfelli, D.Green; "Properties of highly porous hydroxyapatite obtained by the gelcasting of foams," Journal of the American Ceramic Society, **83**, 3021-24 **(2000)**.

[18] S.Padilla, J.Roman, M.V.Regi; "Synthesis of porous hydroxyapatite by combination of gelcasting and foams burn out methods," Journal of Materials Science: Materials in Medicine, **13**, 1193-7 **(2002)**.

[19] C.Bartuli, E.Bemporad, J.M.Tulliani, J.Tirillò, G.Pulci, M.Sebastiani; "Mechanical properties of cellular ceramics obtained by gel casting: Characterization and modeling," Journal of the European Ceramic Society, **29**, 2979-89 **(2009)**.

[20] Z.Sadeghian, J.G.Heinrich, F.Moztarzadeh; "Influ-

Full Paper

ence of powder pre-treatments and milling on dispersion ability of aqueous hydroxyapatite-based suspensions," Ceram.Int., **32,** 331–337 **(2006)**.

[21] S.Nayak, B.P.Singh, L.Besra, T.K.Chongdar, N.M.Gokhale, S.Bhattacharjee; "Aqueous tape casting using organic binder: A case study with YSZ," J.Am.Ceram.Soc., **94**, 3742–3747 **(2011)**.

[22] C.G.Biliaderis; "Structures and phase transitions of starch polymers," In Polysaccharide Association Structures in Food, (ed), R.H.Walter.Marcel Dekker, New York, 57–168 **(1998)**.

[23] J.R.Daniel, R.L.Whistler; "Starch: sources and processing," In Encyclopaedia of Food Science, Food Technology, and Nutrition, (ed), R.Macrae, R.K.Robinson and M.J.Sadler.Academic Press, London, 4377–4380 **(1993)**.

[24] S.Woottichaiwat, S.Puajindanetr, S.M.Best; "Fabrication of porous hydroxyapatite through combination of sacrificial template and direct foaming techniques," Eng.J., **15**, 1-15 **(2011)**.

[25] E.Landi, G.Celotti, G.Logroscino, A.Tampieri; "Carbonated hydroxyapatite as bone substitute," Journal of the European Ceramic Society, **23**, 2931–37 **(2003)**.

[26] T.Y.Yang, J.M.Lee, S.Y.Yoon, H.C.Park; "Hydroxyapatite scaffolds processed using a TBA-based freeze-gel casting/polymer sponge technique," J.Mater.Sci: Mater.Med., **21**, 1495–502 **(2010)**.

[27] J.Zhang, H.Tanaka, F.Ye, D.Jiang, M.Iwasa; "Colloidal processing and sintering of hydroxyapatite," Materials Chemistry and Physics, **101**, 69–76 **(2007)**.

[28] S.Padilla, R.Garcia-Carrodeguas, M.Vallet-Regý; "Hydroxyapatite suspensions as precursors of pieces obtained by gelcasting method," Journal of the European Ceramic Society, **24**, 2223–32 **(2004)**.

[29] A.J.Ruys, K.A.Zeigler, O.C.Standard, A.Brandwood, B.K.Milthorpe, C.C.Sorrel; "Hydroxyapatite sintering phenomena: densiûcation and dehydration behaviour," in: M.J.Bannister (Ed.), Ceramics: Adding The Value, Proceedings of the International Ceramic Conference, Austceram 92, CSIRO, Melbourne, **2**, 605–610 **(1992)**.

[30] A.J.Ruys, M.Wei, C.C.Sorrell, M.R.Dickson, A.Brandwood, B.K.Milthorpe; "Sintering effects on the strength of hydroxyapatite" Biomaterials, **16**, 409-15 **(1995)**.

[31] R.Z.Le Geros, O.R.Trautz, J.P.LeGeros, E.Klein, W.P.Sirra; "Apatite crystallites: effect of carbonate on morphology," Science,**158**, 1409-11 **(1967)**.

[32] T.S.Sampath Kumar, I.Manjubala, J.Gunasekaran; "Synthesis of carbonated calcium phosphate ceramics using microwave irradiation," Biomaterials, **21**, 1623-29 **(2000)**.

[33] G.Xu, I.A.Aksay, J.T.Groves; "Continuous crystalline carbonate apatite thin films," A Biomimetic Approach, J.Am.Chem.Soc., **123**, 2196-203 **(2001)**.

[34] K.Lin, J.Chang, R.Cheng, M.Ruan; "Hydrothermal microemulsion synthesis of stoichiometric single crystal hydroxyapatite nanorods with mono-dispersion and narrow-size distribution," Mater.Lett., **61**, 1683-7 **(2007)**.

[35] Y.Sun, G.Guo, Z.Wang, H.Guo; "Synthesis of single-crystal HAP nanorods Ceram.Int., **32**, 951-4 **(2006)**.

[36] G.Felício-Fernandes, M.C.M.Laranjeira; "Calcium phosphate biomaterials from marine algae, Hydrothermal synthesis and characterization," Quim.Nova., **23**, 441-6 **(2000)**.

[37] F.H.Lin, C.J.Liao, K.S.Chen, J.S.Sun, C.P.Lin; "Petal-like apatite formed on the surface of tricalcium phosphate ceramic after soaking in distilled water," Biomaterials, **22**, 2981–92 **(2001)**.

[38] L.L.Hench, J.Wilson; "An Introduction to Bioceramics," World Scientific, London, U.K., **(1993)**.

[39] P.Ducheyne, Q.Qiu; "Bioactive ceramics: the effect of surface reactivity on bone formation and bone cell function," Biomaterials, **20**, 2287–303 **(1999)**.

[40] H.Ghomi, M.H.Fathi, H.Edris; "Preparation of nanostructure hydroxyapatite scaffold for tissue engineering applications," J.Sol-Gel Sci.Technol., **58**, 642–50 **(2011)**.

[41] O.Lyckfeldt, J.M.F.Ferreira; "Processing of porous ceramics by 'starch consolidation'," Journal of the European Ceramic Society, **18**, 131-40 **(1998)**.

[42] M.A.Janney; "Method for molding ceramic powders," US Patent, **4894**, 194, **(1990)**.

[43] W.Chen, X.Zhang, J.Wang, X.Zhao; "Biomedical materials research in the far east", (Eds), by X.Zhao and Y.Ikada (Kobunshi Kankokai, Tokyo), 157-158 **(1993)**.

[44] D.M.Liu; "Fabrication of hydroxyapatite ceramic with controlled porosity," J.of Materials Science: Materials in Medicine, **8**, 227-32 **(1997)**.

[45] Y.Zhang, L.Hao, M.M.Savalani, R.A.Harris, K.E.Tanne; "Characterization and dynamic mechanical analysis of selective laser sintered hydroxyapatite-ûlled polymeric composites," Journal of Biomedical Materials Research Part A, **86A(3)** 607–16 **(2008)**.

Full Paper

[46] T.Kokubo, H.Kushitani, S.Sakka, T.Kitsugi, T.Yamamuro; "Solutions able to reproduce in vivo surface-structure changes in bioactive A-W glass-ceramic," J.Biomed.Mater.Res., **24**, 721–34 **(1990)**.

[47] V.Karageorgiou, D.Kaplan; "Porosity of 3D biomaterial scaffolds and osteogenesis," Biomaterials, **26**, 5474–91 **(2005)**.

[48] H.Yuan, K.Kurashina, J.D.de-Bruijn, Y.B.Li, K.de-Groot, X.D.Zhang; "A preliminary study on osteoinduction of two kinds of calcium phosphate ceramics," Biomaterials, **20**, 1799–806 **(1999)**.

[49] A.Krajewski, A.Ravaglioli, E.Roncari, P.Pinasco; "Porous ceramic bodies for drug delivery," J.Mater.Sci.Mater.Med., **12**, 763-71 **(2000)**.

[50] H.Yokozeki, T.Hayashi, T.Nakagawa, H.Kurosawa, K.Shibuya, K.Ioku; "Influence of surface microstructure on the reaction of the active ceramics in vivo," J.Mater.Sci.Mater.Med., **9**, 381-4 **(1998)**.

[51] A.Tampieri, G.Celotti, S.Sprio, A.Delcogliano, S.Franzese; "Porosity-graded hydroxyapatite ceramics to replace natural bone," Biomaterials, **22**, 1365-70 **(2001)**.

[52] S.K.Swain, S.Bhattacharyya, D.Sarkar; "Preparation of porous scaffold from hydroxyapatite powders," Materials Science and Engineering, **C31**, 1240–44 **(2011)**.

[53] G.Tripathi, B.Basu; "A porous hydroxyapatite scaffold for bone tissue engineering: Physico-mechanical and biological evaluations," Ceramics International, **38**, 341–9 **(2012)**.

[54] Y.Zhang, M.Zhang; "Three dimensional macroporous calcium phosphate bioceramics with nested chitosan sponges for load bearing implants," J.Biomed.Mater.Res., **61**, 1–8 **(2002)**.

[55] I.Sopyan, M.Mel, S.Ramesh, K.A.Khalid; "Porous hydroxyapatite for artiûcial bone applications," Science and Technology of Advanced Materials, **8**, 116–23 **(2007)**.

[56] H.Yoshikawa, A.Myoui; "Bone tissue engineering with porous hydroxyapatite ceramics," J.Artif.Organs., **8**, 131-6 **(2005)**.